

Mechanical Behavior of Grafts for Coronary Artery Bypass Surgery

Jan Veselý, Lukáš Horný, Hynek Chlup, Rudolf Žitný

Vedoucí práce: prof. Ing. Rudolf Žitný, CSc.

Abstrakt

Aortokoronární bypass je v dnešní době standardní technika používaná k obnovení průchodu krve věnčitými tepnami. Segment velké skryté žíly (vena saphena magna) je nejčastěji používán jako štěp, který přemostuje zúžené (ucpané) místo uvnitř koronární tepny. 15 vzorků skrytých žil bylo podrobeno inflačně-extenzním testům, za účelem charakterizace mechanického chování. Experimentální data byla nafitována nelineárním anizotropním konstitutivním modelem, pro obdržení materiálových parametrů žilních štěpů. Bylo zjištěno, že při nízkých zatěžovacích tlacích (do cca 2.5 kPa) jsou žíly velice deformovatelné. Toto prvotní chování je pro vyšší hodnoty tlaku vystřídáno výrazně tužší odezvou materiálu. Získané materiálové parametry mohou být využity jako vstupní hodnoty do numerických výpočtů simulujících chování aortokoronárního bypassu.

Key words:

Anisotropy, bypass graft, collagen, constitutive model, saphenous vein.

1. Introduction

Coronary artery disease (CAD) is the most important cause of morbidity and mortality worldwide. In 2013 CAD globally resulted in 8.14 million deaths (16.8%) up from 5.74 million deaths (12%) in 1990 (GBD 2013). The coronary artery bypass graft surgery (CABG) is the standard procedure to treat this disease, Fig. 1. Although arterial grafts are preferred as bypass conduits because of their better patency rates, their use is limited because of the length and number of available segments. Therefore, the saphenous vein (SV) is most often used as an arterial bypass graft in the coronary circulation (Athanasίου et al., 2011). However, its patency is relatively low (less than 50% in 10 years) compared with the patency rate of arterial grafts (Fitzgibbon et al., 1996).

Saphenous veins' properties are, however, optimized for a mechanical environment very different from arterial conditions. Immediately after the surgery, remodeling processes are triggered and the vein adapts to the elevated blood pressure, flow rate and oscillatory wall shear stress. As an undesirable effect of the changed conditions, the patency of the graft may be substantially compromised by an intimal hyperplasia or thrombosis (Fitzgibbon et al., 1996; Hwang et al., 2012).

Much work is now being done to deepen our knowledge of the mechanobiology of graft remodeling, but this process is still not completely understood (Tran-Son-Tay et al., 2008; Hwang et al., 2012; Hwang et al., 2013; Sassani et al., 2013). The adaptation to the changed conditions leads not only to a change in the diameter and thickness of the graft wall, but also to a changed internal structure and thus a change in the constitutive equation expressing the mutual relation between stress and strain (Hwang et al., 2012).

In contrast to the work done on arteries, there have been only a few papers describing the multi-axial mechanical response of veins within the framework of nonlinear elasticity (Desch

and Weizsäcker, 2007; Cacho et al., 2007; McGilvray et al., 2010; Sokolis, 2013; Zhao et al., 2007). Probably, the most comprehensive study of mechanical properties of saphenous veins has been provided by Donovan et al. (1990). They however used a uniaxial tensile test, which imposes certain limitations on their data when used to construct 3D constitutive equations of a nonlinear anisotropic material (Holzapfel, 2006). There are also papers reporting pressure–diameter relationships, but without arriving at the constitutive equations (Stocker et al., 2003; Wesly et al., 1975).

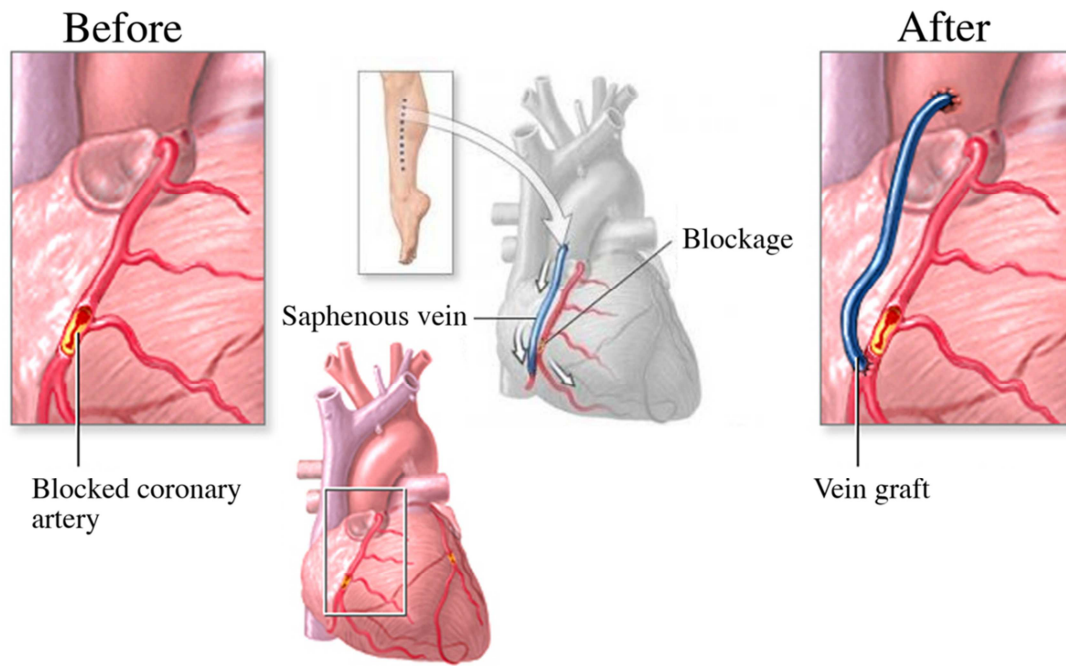


Fig. 1. Coronary artery bypass graft surgery. The place of blockage is overbridged by the venous graft. Adopted from <http://www.adamimages.com/>.

In last decade, the development of numerical computation methods enables to perform simulations to model different phenomena in human body including bypass graft surgery. There are numerous studies available in the literature focusing on anastomotic flow dynamics, see, e.g., Migliavacca and Dubini (2005). Surprisingly, however, there are only very few studies available dealing with the related solid mechanics (Ballyk et al., 1998; Gu et al., 2006; Leuprecht et al., 2002), and the fluid–structure interaction (Leuprecht et al., 2002, Hofer et al., 1996) of bypass grafts. The quality of the experimentally-determined mechanical properties of the tissue involved in the simulation is a crucial factor to obtain relevant results (Cacho et al., 2007).

The main goal of this study is to find constitutive equations for the multi-axial state of stress suitable for describing the passive nonlinear anisotropic mechanical behavior of human vena saphena magna. Our approach is based on the strain energy density function suggested by Holzapfel et al. (2000). Experimental data were obtained in ex vivo inflation tests (with free axial extension) conducted with samples obtained from fifteen donors.

2. Materials and Methods

2.1 Material

Human great saphenous veins for inflation-extension tests were collected either during coronary-artery bypass surgery conducted at the General University Hospital in Prague (obtained with informed consent) or during autopsies conducted at the Department of

Forensic Medicine of the Third Faculty of Medicine of Charles University in Prague within 24 hours after death. The experimental protocol was approved by the institutional Ethical Committees. Collected veins were placed in the physiological solution and tested in less than three hours after excision. The segment of the vein without side branches and of minimal length 40 mm was cut from a body. Surrounding connective tissue and fat were removed from the graft material before mechanical testing. Only the veins with no substantial deviation from circular cylindrical geometry were included into the study. Prior to the mechanical testing, two rings were cut out from the tissue at both ends, and the mean reference dimensions of the samples (external radius, thickness) were determined by means of image analysis of digital photographs (Nis-Elements, Nikon Instruments Inc., NY, USA).

2.2 Inflation-extension test

Each specimen was marked with a black liquid eye-liner, cannulated at one end and hung vertically in the experimental setup (Fig. 2). The experimental protocol consisted of four pre-cycles to stabilize the mechanical response (preconditioning), and a fifth cycle was used in the data analysis. Pressurization was performed in the range from 0 up to ≈ 15 kPa using a motorized syringe (Standa Ltd, Vilnius, Lithuania). The intraluminal pressure was monitored by pressure transducer (sample rate 500 Hz) (Cressto s.r.o, Czech Republic). The deformed geometry was recorded by a CCD camera with frequency 20 Hz (Dantec Dynamics, Skovlunde, Denmark). In the data post processing, changes in the length between the black marks (Fig. 2) and average changes in the silhouette (also between the marks to avoid end effects) were determined by the edge detection algorithm in Matlab (MathWorks, MA, USA). They were used to compute axial stretch ratio λ_z and circumferential stretch ratio at the outer radius $\lambda_\theta(r_o)$. All experiments were performed at room temperature (22°C).

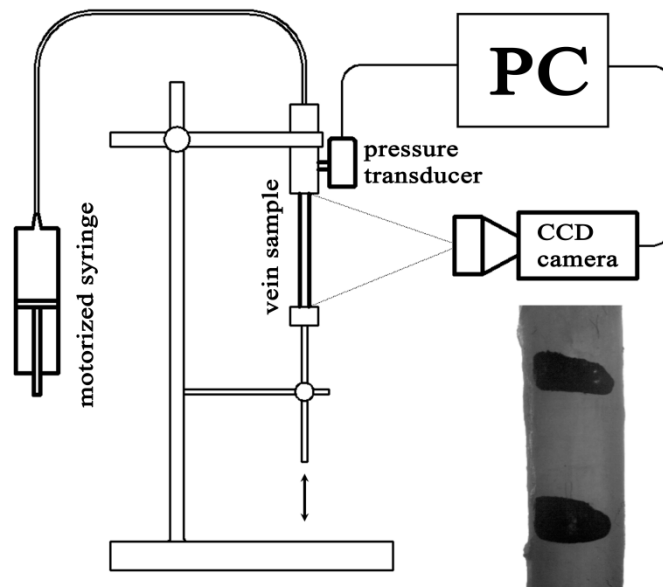


Fig. 2. Experimental inflation-extension test set-up, and a picture of the sample taken with a CCD camera. The black marks were used to identify the longitudinal deformation. Adopted from Veselý et al. (2015).

2.3 Kinematics

The vein was considered to be a homogeneous, incompressible cylindrical thick-walled tube. The kinematics of the experiment was modeled as simultaneous inflation and extension, in

which the material particle located in the reference (stress free) configuration in the position $X = (R, \Theta, Z)$ is mapped by the deformation into the position $x = (r, \theta, z)$ in the current configuration, according to equation (1).

$$r = r(R) \quad \theta = \Theta \quad z = \lambda_z Z \quad (1)$$

The situation is depicted in Fig. 3. Here R_o and R_i respectively denote the outer and inner radius in the reference configuration ($R_i \leq R \leq R_o$) and r_o and r_i in the deformed configuration ($r_o \leq r \leq r_i$). By analogy, H and L ($0 \leq Z \leq L$) and h and l ($0 \leq z \leq l$) denote its thickness and length measured between the marks.

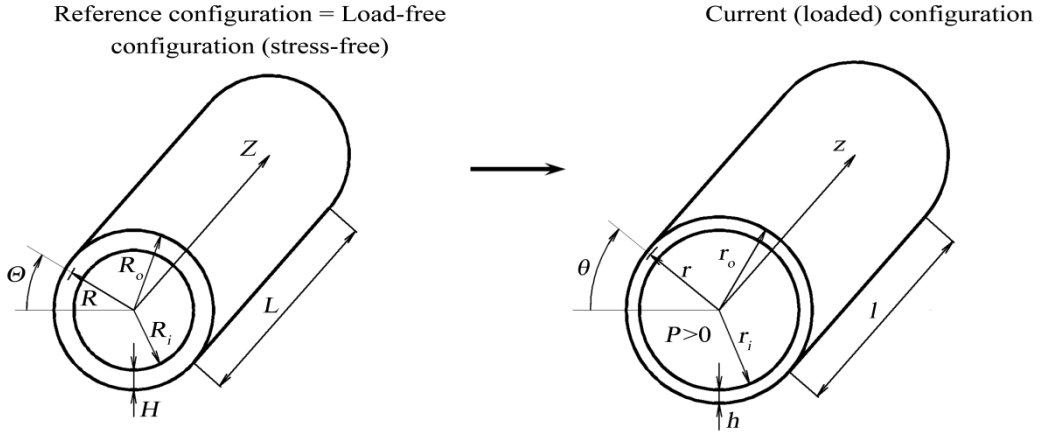


Fig. 3. Kinematics of the deformation of the vein wall. The stress-free configuration (assumed to be the same as the load-free configuration) and the deformed current (loaded) configuration are depicted. Adopted from Veselý et al. (2015).

The deformation gradient is then described by equation (2). Here the longitudinal stretch ratio was considered to be uniform. The assumption of incompressibility is expressed via the kinematical constraint $\det \mathbf{F} = 1$, which allows us to write λ_r also as $\lambda_r = 1/(\lambda_z \lambda_\theta)$.

$$\mathbf{F} = \begin{pmatrix} \lambda_r(r) & 0 & 0 \\ 0 & \lambda_\theta(r) & 0 \\ 0 & 0 & \lambda_z \end{pmatrix} = \begin{pmatrix} \frac{\partial r}{\partial R} & 0 & 0 \\ 0 & \frac{r}{R} & 0 \\ 0 & 0 & \frac{l}{L} \end{pmatrix} \quad (2)$$

It is useful to express the incompressibility condition by means of the radius and the length:

$$\pi L (R_o^2 - R_i^2) = \pi l (r_o^2 - r_i^2) \quad (3)$$

This was used to compute the inner radius during the deformation. From here, substituting R_i by R and r_i by r , we also arrive at $R = R(r)$ required in $\lambda_\theta(r)$ expression.

2.4 Constitutive model

The material of venous wall was considered to be an anisotropic hyperelastic continuum characterized by the strain energy density function W proposed by Holzapfel et al. (2000). The strain energy density function is expressed by equation (4).

$$W = W_{isotropic} + W_{anisotropic} = \frac{\mu}{2} (I_1 - 3) + \frac{k_1}{2k_2} \sum_{i=4,6} \{ \exp[k_2 (I_i - 1)^2] - 1 \} \quad (4)$$

In (4) μ and k_1 are stress-like parameters, k_2 is dimensionless parameter. I_1 is the first invariant of the right Cauchy-Green strain tensor and I_4 is additional invariant arising from

material anisotropy and has the meaning of square of the stretch in preferred (fiber) direction. I_1 and I_4 are defined in (5) and (6).

$$I_1 = \lambda_r^2 + \lambda_\theta^2 + \lambda_z^2 \quad (5)$$

$$I_4 = I_6 = \lambda_\theta^2 \cos^2 \beta + \lambda_z^2 \sin^2 \beta \quad (6)$$

In (6) β defines preferred direction within the material measured from circumferential axis of the tube in stress-free configuration of the vein.

Finally, the constitutive equation for an incompressible hyperelastic material can be written in the form of (7). Here $\boldsymbol{\sigma}$ denotes the Cauchy stress tensor and p is an undetermined multiplier induced by incompressibility constraint.

$$\boldsymbol{\sigma} = 2\mathbf{F} \frac{\partial W}{\partial \mathbf{C}} \mathbf{F}^T - \mathbf{I}p \quad (7)$$

2.5 Thick-walled tube model

Let us denote as \widehat{W} the strain energy density function (4) with eliminated explicit dependence on λ_r by substituting $\lambda_r = 1/(\lambda_\theta \lambda_z)$. Considering the boundary conditions $\sigma_{rr}(r_i) = -P$ and $\sigma_{rr}(r_o) = 0$, the equilibrium equations in the radial and axial direction have the form (8) and (9), respectively. Here P denotes internal pressure and F_{red} is the reduced axial (prestretching) force acting on the closed end of the tube additionally to the force generated by the pressure acting on the end (Horny et al., 2014a; Horny et al., 2014b; Matsumoto and Hayashi, 1996).

$$P = \int_{r_i}^{r_o} \lambda_\theta \frac{\partial \widehat{W}}{\partial \lambda_\theta} \frac{dr}{r} \quad (8)$$

$$F_{red} = \pi \int_{r_i}^{r_o} \left(2\lambda_z \frac{\partial \widehat{W}}{\partial \lambda_z} - \lambda_\theta \frac{\partial \widehat{W}}{\partial \lambda_\theta} \right) r dr \quad (9)$$

2.6 Determination of the material parameters

The material parameters (μ , k_1 , k_2 , β) of the constitutive model were determined by fitting model predictions based on (8) and (9) to the experimental data. The objective function Q (10) was minimized in Maple (Maplesoft, Waterloo, Canada). P^{mod} and P^{exp} in (10) denote the internal pressure predicted by (8) and measured experimentally, respectively. The same denotation applies for axial force F_{red} . Neglecting the small weight of the tube's lower plug ($\approx 5g$), F_{red}^{exp} was considered to be 0. w_P and w_F are weight factors. n is the number of observation points.

$$Q = \sum_{i=1}^n \left\{ \left[w_P (P_i^{mod} - P_i^{exp})^2 \right] + \left[w_F (F_{red i}^{mod} - F_{red i}^{exp})^2 \right] \right\} \quad (10)$$

3. Results

The data collected in the experiments are summarized in Table 1. Column $Mean(|F_{red}^{mod}|)$ shows how accurately the axial force was predicted by the model ($F_{red}^{exp} = 0$). Eleven samples of human saphenous vein were collected during surgery (mean \pm SD; age 55 ± 15 ; 7 male and 4 female; 3 donors with varicose disease) and four in autopsy (age 65 ± 5 ; 3 male and 1 female; one with varicose disease). Fig. 4 shows the loading part of the fifth inflation-extension cycle to which the constitutive models were fitted. Model predictions were obtained by substituting the estimated parameters into the system (8) and (9), and are depicted by continuous curves (donors with varicose disease are in blue). The models predict satisfactorily the experimental pressure-stretch data (Fig. 4 upper panel). However, the predicted axial

stretch, shown in Fig. 4 (bottom panel), corresponds to the experiments only to a limited extent.

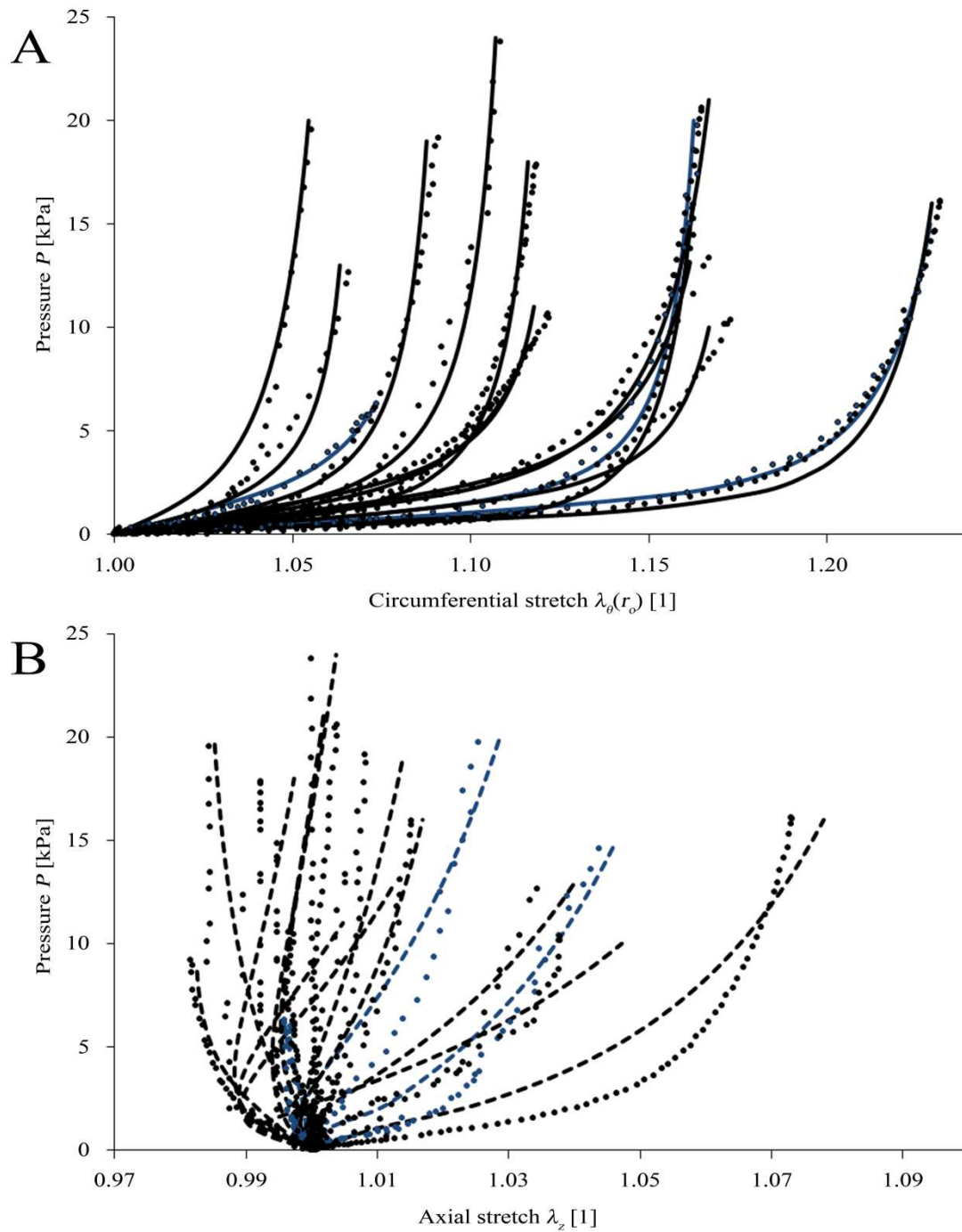


Fig. 4. The resulting pressure-circumferential stretch at the outer radius (panel A) and pressure-axial stretch (panel B) dependences. The experimental data (dotted curves) are compared with data predicted by the constitutive model (solid curves). The donors with varicose disease are in blue. The interval in axial stretch from 0.99 to 1.01 in panel B identified by gray lines represents bounds of uncertainty caused by resolution of digital cameras. Adopted from Veselý et al. (2015).

Table 1. – Age and sex of the donors (F stands for female and M for male), obtained material parameters (μ , k_1 , k_2 , β), and computed mean force during pressurization $Mean(|F_{red}^{mod}|)$ for each sample of vein. Adopted from Veselý et al. (2015).

| Donor | Age [years] | Sex | R_o [mm] | H [mm] | Material parameters | | | | $Mean(F_{red}^{mod})$ [N] | Pathology |
|---------|-------------|-----|------------|----------|---------------------|-------------|-----------|-------------|-----------------------------|-----------|
| | | | | | μ [kPa] | k_1 [kPa] | k_2 [-] | β [°] | | |
| CABG | | | | | | | | | | |
| a | 63 | M | 2.89 | 0.83 | 5.5 | 4.0 | 61.7 | 40.3 | 9.1E-08 | - |
| | 66 | F | 2.12 | 0.49 | 28.4 | 8.4 | 122.1 | 39.3 | 2.6E-08 | varicose |
| | 27 | F | 2.32 | 0.88 | 4.0 | 1.5 | 18.2 | 43.0 | 7.0E-08 | varicose |
| | 42 | F | 2.78 | 0.80 | 5.7 | 1.4 | 13.5 | 43.1 | 1.8E-07 | varicose |
| | 69 | M | 1.14 | 0.59 | 4.2 | 3.0 | 10.8 | 44.1 | 8.7E-09 | - |
| b | 63 | M | 2.05 | 0.76 | 5.6 | 4.5 | 13.6 | 42.7 | 4.5E-08 | - |
| a | 60 | M | 1.80 | 0.53 | 9.9 | 5.9 | 62.2 | 39.8 | 4.4E-08 | - |
| | 76 | M | 1.98 | 0.57 | 7.0 | 19.3 | 48.2 | 36.5 | 3.8E-08 | - |
| | 50 | M | 2.33 | 0.57 | 30.7 | 30.3 | 330 | 38.4 | 5.5E-08 | - |
| b | 60 | M | 1.92 | 0.47 | 13.7 | 9.3 | 85.5 | 38.2 | 6.7E-08 | - |
| | 49 | F | 1.86 | 0.39 | 14.1 | 4.2 | 43.2 | 41.2 | 2.9E-08 | - |
| Autopsy | | | | | | | | | | |
| c | 72 | F | 1.78 | 0.71 | 3.1 | 2.3 | 8.8 | 42.6 | 2.5E-08 | - |
| | 60 | M | 0.92 | 0.28 | 9.5 | 5.0 | 53.5 | 41.5 | 6.4E-09 | - |
| | 60 | M | 2.14 | 0.42 | 4.4 | 1.4 | 50.5 | 40.4 | 5.9E-08 | - |
| | 68 | M | 1.80 | 0.48 | 4.2 | 1.0 | 13.1 | 41.9 | 6.1E-08 | varicose |

4. Discussion and Conclusions

In our study, overloading inflation-extension test was performed on samples of human saphenous vein. The experimental data was fitted by the hyperelastic nonlinear anisotropic constitutive model proposed by Holzapfel et al. (2000). Only the passive mechanical response was modeled.

Fig. 4 shows that the vein under simultaneous inflation and extension exhibit significantly smaller deformations in axial direction than in circumferential direction. This finding is in agreement with results of Wesley et al. (1975), who studied the pressure-strain relationship of dog jugular and human saphenous veins. Specifically, in our study measured axial stretches are generally in the range from 0.98 to 1.03. For samples M50, M63a, F49, M60a, F69, F66V, M60d and M63b, the range of axial deformation during the entire pressurization period was not higher than approx. 1%. This small deformation is, however, determined with relatively high measurement uncertainty, caused by the resolution of CCD camera. Due to this fact axial stretches in the interval from 0.99 to 1.01 are affected by experimental uncertainty which is in Fig. 4 highlighted by gray lines.

Four donors with diagnosed varicose disease were included in this study in order to reveal differences in mechanical response in comparison with healthy donors. However, we were able to obtain only four samples which is a small number for statistical evaluation and these samples do not appear to behave differently. Finally, we preserved them in the study, because obtained material parameters could be used by other authors.

To the best of our knowledge, this is the first study which presents a comprehensive set of material parameters for human saphenous veins modeled as the thick wall tube suitable for describing multi-axial stress states. They can be helpful as input in numerical simulations of the remodeling and adaptation processes triggered after bypass surgery involving autologous vein grafts (Hwang et al., 2012, 2013; Sassani et al., 2013).

List of symbols

| | | |
|-----------------------|--|-------|
| R_o | reference outer radius of the vein sample | (mm) |
| R_i | reference inner radius of the vein sample | (mm) |
| r_o | deformed outer radius of the vein sample | (mm) |
| r_i | deformed inner radius of the vein sample | (mm) |
| H | reference thickness of the vein sample | (mm) |
| h | deformed thickness of the vein sample | (mm) |
| λ_r | stretch ratio in radial direction | (1) |
| λ_θ | stretch ratio in circumferential direction | (1) |
| λ_z | stretch ratio in axial direction | (1) |
| \mathbf{F} | deformation gradient | (-) |
| L | reference length of the vein sample | (mm) |
| l | deformed length of the vein sample | (mm) |
| W | strain energy density function | (kPa) |
| I_1 | first invariant of the right Cauchy-Green strain tensor | (1) |
| I_4 | fourth invariant of the right Cauchy-Green strain tensor | (1) |
| μ | constitutive model parameter | (kPa) |
| k_1 | constitutive model parameter | (kPa) |
| k_2 | constitutive model parameter | (1) |
| β | constitutive model parameter | (rad) |
| $\boldsymbol{\sigma}$ | Cauchy stress tensor | (-) |
| \mathbf{I} | second order unit tensor | (-) |
| p | Lagrange multiplier | (kPa) |
| P | intraluminal pressure | (kPa) |
| F_{red} | reduced axial (prestretching) force | (N) |

Acknowledgement

This study has been supported by Czech Ministry of Health grant no. NT 13302.

References

- Athanasiou, T., Saso, S., Rao, C., Vecht, J., Grapsa, J., Dunning, J., Lemma, M., Casula, R., 2011. Radial artery versus saphenous vein conduits for coronary artery bypass surgery: forty years of competition—which conduit offers better patency? A systematic review and meta-analysis. *European Journal Cardiothoracic Surgery* 40, 208–220.
- Ballyk, P.D., Walsh, C., Butany, J., Ojha, M., 1998. Compliance mismatch may promote graft-artery intimal hyperplasia by altering suture-line stresses. *Journal of Biomechanics* 31, 229-237.
- Cacho, F., Doblaré, M., Holzapfel, G.A., 2007. A procedure to simulate coronary artery bypass graft surgery. *Medical and Biological Engineering and Computing* 45, 819-827.
- Desch, G. W. Weizsäcker, H. W., 2007. A model for passive elastic properties of rat vena cava. *Journal of Biomechanics* 40, 3130-3145.
- Donovan, D.L., Schmidt, S.P., Townshend, S.P., Njus, G.O., Sharp, W.V., 1990. Material and structural characterization of human saphenous vein. *Journal of Vascular Surgery* 12, 531-537.
- FitzGibbon, G. M., Kafka, H. P., Leach, A. J., Keon, W. J., Hooper, G. D., Burton, J. R., 1996. Coronary bypass graft fate and patient outcome: Angiographic follow-up of 5,065

- grafts related to survival and reoperation in 1,388 patients during 25 years. *Journal of the American College of Cardiology* 28, 616-626.
- GBD 2013 Mortality and Causes of Death, Collaborators (17 December 2014). "Global, regional, and national age-sex specific all-cause and cause-specific mortality for 240 causes of death, 1990-2013: a systematic analysis for the Global Burden of Disease Study 2013."
- Gu, H., Chua, A., Tan, B.K., Chew, H.K., 2006. Nonlinear finite element simulation to elucidate the efficacy of slit arteriotomy for end-to-side arterial anastomosis in microsurgery. *Journal of Biomechanics* 39, 435–443.
- Hofer, M., Rappitsch, G., Perktold, K., Trubel, W., Schima, H., 1996. Numerical study of wall mechanics and fluid dynamics in end-to-side anastomoses and correlation to intimal hyperplasia. *Journal of Biomechanics* 29, 1297–1308.
- Holzapfel, G.A., Gasser, T.C., Ogden, R.W., 2000. A new constitutive framework for arterial wall mechanics and a comparative study of material models. *Journal of Elasticity* 61, 1-48.
- Holzapfel, G. A., 2006. Determination of material models for arterial walls from uniaxial extension tests and histological structure. *Journal of Theoretical Biology* 238, 290-302.
- Horný, L., Netušil, M., Voňavková, T., 2014a. Axial prestretch and circumferential distensibility in biomechanics of abdominal aorta. *Biomechanics and Modeling in Mechanobiology* 13, 783-799.
- Horný, L., Netušil, M., Daniel, M., 2014b. Limiting extensibility constitutive model with distributed fibre orientations and ageing of abdominal aorta. *Journal of the Mechanical Behavior of Biomedical Materials* 38, 39-51.
- Hwang, M., Berceci, S. A., Garbey, M., Kim, N. H., Tran-Son-Tay, R., 2012. The dynamics of vein graft remodeling induced by hemodynamic forces: A mathematical model. *Biomechanics and Modeling in Mechanobiology*, 11, 411-423.
- Hwang, M., Garbey, M., Berceci, S. A., Wu, R., Jiang, Z., Tran-Son-Tay, R., 2013. Rule-based model of vein graft remodeling. *PLoS ONE* 8, e57822.
- Leuprecht, A., Perktold, K., Prosi, M., Berk, T., Trubel, W., Schima, H., 2002. Numerical study of hemodynamics and wall mechanics in distal end-to-side anastomoses of bypass grafts. *Journal of Biomechanics* 35, 225–236.
- Matsumoto, T., Hayashi, K., 1996. Stress and strain distribution in hypertensive and normotensive rat aorta considering residual strain. *Journal of Biomechanical Engineering* 118, 62-71.
- McGilvray, K. C., Sarkar, R., Nguyen, K., Puttlitz, C. M., 2010. A biomechanical analysis of venous tissue in its normal and post-phlebotic conditions. *Journal of Biomechanics* 43, 2941-2947.
- Migliavacca, F., Dubini, G., 2005. Computational modeling of vascular anastomoses. *Biomechanics and Modeling in Mechanobiology* 3, 235–250.
- Sassani, S. G., Theofani, A., Tsangaris, S., Sokolis, D. P., 2013. Time-course of venous wall biomechanical adaptation in pressure and flow-overload: Assessment by a microstructure-based material model. *Journal of Biomechanics* 46, 2451-2462.
- Sokolis, D. P., 2013. Experimental investigation and constitutive modeling of the 3D histomechanical properties of vein tissue. *Biomechanics and Modeling in Mechanobiology* 12, 431-451.

Stooker, W., Gök, M., Sipkema, P., Niessen, H.W.M., Baidoshvili, A., Westerhof, N., Jansen, E.K., Wildevuur, C.R.H., Eijnsman, L. , 2003. Pressure-Diameter Relationship in the Human Greater Saphenous Vein. *Annals of Thoracic Surgery* 76, 1533-1538.

Tran-Son-Tay, R., Hwang, M., Garbey, M., Jiang, Z., Ozaki, C. K., Berceci, S. A., 2008. An experiment-based model of vein graft remodeling induced by shear stress. *Annals of Biomedical Engineering* 36, 1083-1091.

Vesely, J., Horný, L., Chlup, H., Adámek, T., Krajíček, M., Žitný, R., 2015. Constitutive modeling of human saphenous veins at overloading pressures. *Journal of the Mechanical Behavior of Biomedical Materials* 45, 101-108.

Wesly, R.L.R., Vaishnav, R.N., Fuchs et, a.J.C.A., Patel, D.J., Greenfield Jr., J.C., 1975. Static linear and nonlinear elastic properties of normal and arterialized venous tissue in dog and man. *Circulation Research* 37, 509-520.

Zhao, J., Jesper Andreasen, J., Yang, J., Steen Rasmussen, B., Liao, D., Gregersen, H., 2007. Manual pressure distension of the human saphenous vein changes its biomechanical properties - implications for coronary artery bypass grafting. *Journal of Biomechanics* 40, 2268-2276.